**Journal of Computational and Applied Research
in Mechanical Engineering**

jcarme.sru.ac.ir

SRTTU

JCARME

ISSN: 2228-7922

Research paper

Dynamic analysis of multi-body dynamics model of mold oscillator including self-excitation of supporting system

Y. H. Park[*]

Department of Mechanical Engineering, Sunmoon University, Asan, Republic of Korea

Abstract

A hydraulically driven mold oscillator challenges estimating the dynamic state variables precisely. Significantly, the additional stiffness effect of hydraulic oil is variable according to operating conditions, and it is hard to formulate it as a mathematical expression. This study investigates the dynamic characteristics of a mold oscillator operated by two hydraulic cylinders with other springs and dampers to determine the non-linear effect and estimate exact dynamic state variables to improve the accuracy control. The mold oscillator is excited in either step oscillation or sine-sweeping oscillation to measure its dynamic behaviors, including mold displacement and hydraulic cylinder pressure. Due to non-linear properties, the dynamic behavior change according to excitation conditions during sine-sweeping oscillation. Primarily, peak frequencies around 50 Hz are found from experimental pressure-displacement data in the frequency domain. To identify the oscillating mechanisms, equivalent 1-DOF and 2-DOF mass-damper-spring models for the mold oscillator are established. The fundamental system property is derived by experiment and a finite element multi-body dynamics model. In addition, inverse dynamics and numerical analysis are applied to derive the unknown force from the hydraulic servo system and structural characteristics. The unknown force is related to a friction problem and an elastic deflection by relative components near the mold. For high accuracy control, the unknown force model by an additional mass-spring model that causes high-frequency vibrations at 49, 48, 47, 46, or 45 Hz is suggested to formulate the equation of motion with the additional vibrations without any arbitrary modeling process.

1. Introduction

Many applications for lifting a heavy mold oscillator, maintaining constant continuous casting speed and suppling homogeneous ingot steel to a rolling strand, have been tried [1-6]. However, hydraulic servo systems have been preferred because of their excellent stiffness characteristics and rapid response to speed or direction changes [7]. However, the hydraulic servo may leak operating oil, cause environmental

problems [8], and cannot be easily modified due to its non-linear input responses. The nonlinearity is caused primarily by the servo valve and the hydraulic cylinder, including the orifice, hydraulic cylinder damping, stiffness, and friction. [9] In previous work on mold oscillation, experimental research was conducted to obtain a detailed design. For example, the relationship between an oscillating signal and lubrication consumption was calculated according to friction between mold and ingot steel [10, 11]. In order to minimize the consequences of non-linear responses, various linearized models for the hydraulic servo system have been developed for small instruments. However, research about the mold oscillating mechanism has not been published because the information is proprietary. In addition, structural analysis, including fitting the beam model parameters to match the actual resonance frequencies exhibited by thin and thick slab casting mold oscillators [12], a novel type of mold oscillator instead of a hydraulic driven system due to its complex and maintenance problem [13], development of an intelligent PID (i-PID) controller for position control of a non-linear electro-hydraulic system [14], development of a new electro-hydraulic power source based on pressure-controlled variable piston pump driven by a servo motor [15], have been considered to improve the accuracy control and the performance. Engineers triy to find good operating conditions in many steel factories by trial and error without having a basic design. Considering that the mold oscillation occurs at low frequency (0.83 ~ 6.67 Hz) and because the oscillating system is mounted on a stable base, the trial-and-error method often gives reasonable solutions. Another method establishes a proper transfer function near the operating point [16]. However, these methods give one solution among various solutions, not necessarily the best one. The system will not be estimated if design variables or operating conditions change. Such changes in conditions are expected in modern steel manufacturing in which high productivity and fast production processes are demanded; rapid casting is essential to meet these demands [17-19]. Mold oscillators should be checked in

many ways, including an assessment of how dynamic characteristics depend on design variables to secure a stable system that is also fast [20-22].

Experimental data and a finite element (FE) multi-body dynamics model are used to establish equivalent 1-DOF and 2-DOF models and analyze the dynamic responses in the time and frequency domains. The difference between the experiment and the numerical solution is investigated to formulate the variable non-linear effect due to the hydraulic cylinder, which was not a concern in the previous work. Significantly, the dynamic responses to natural frequency ω_{nat} and excitation frequency ω_{exc} are primary frequencies. Based on the physical relationship between the primary frequencies, vibrations theories derive the connecting spring stiffness and damper between the mold and the ground and derive a mathematical expression from describing an unknown non-linear force. The primary concern of the present research is to control the system precisely

2. Methods
2.1. Analysis methodology with simplified mold oscillator model
2.1.1. 1-DOF mold oscillator model

Before modeling a system, experiment data, mold displacement, hydraulic cylinder pressure, and design variables according to various oscillating signals are corrected from the monitoring system. The 1-DOF mass-spring-damper system is a simple model representing the mold oscillator, consisting of 2 double-acting cylinders (Fig. 1).
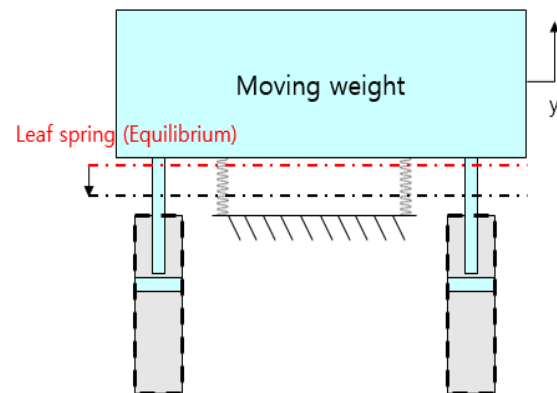

Fig. 1. Mold oscillator.

The mass, damping ratio, and stiffness of the model (Table 1) were derived from the pressure difference in the cylinder when a step signal was applied. These values were used to calculate the force equilibrium between the moving weight, the leaf spring, and the hydraulic cylinder (Eq. (1)):

$$m\ddot{y} + c\dot{y} + (k_{leaf} + k_{add})y - k_{leaf}\, y_{leaf} = F_{pressure} - mg \tag{1}$$

where m is the mass of the mold [kg], c is an equivalent damping coefficient [N/m-s], k_{leaf} is a leaf spring stiffness [N/m], k_{add} is a hydraulic cylinder stiffness [N/m], g is gravity acceleration [m/s^2], $F_{pressure}$ is a hydraulic cylinder pressure force [N].

The mold's numerical solution and experimental displacement show identical distributions to the system properties (Fig. 2).

By using the equivalent 1-DOF model, the numerical solution and the experiment are not the same when a sweeping signal is applied (Fig. 3). In other words, If $F_{pressure}$, the experiment data from the monitoring system, is applied to the equation of motion, the dynamic response, such as the displacement, cannot be represented as a sine-sweeping signal.

Table 1. Mold oscillator configuration.

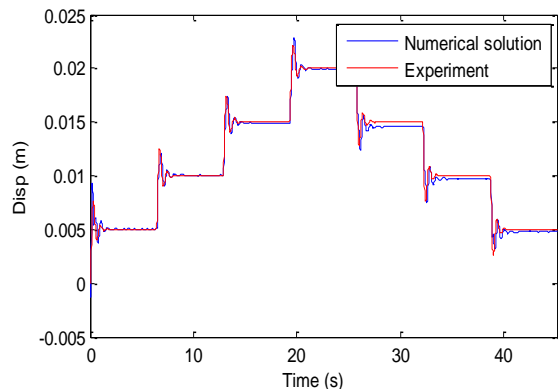| Quantity	Value
M : Mass	33 ton
ζ : Damping ratio	0.3
K : Total stiffness	8,287,639 N/m

Fig. 2. Comparison between the numerical solution and experiment about displacement with a step input signal.
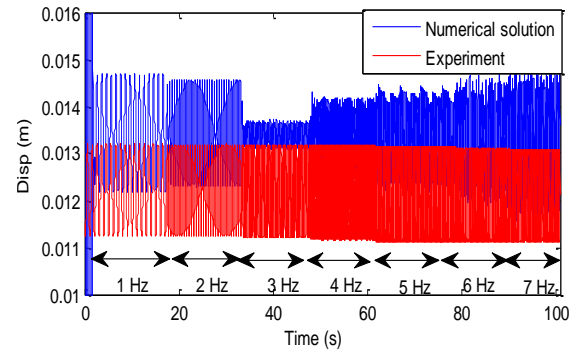

Fig. 3. Comparison between the numerical solution and experiment about displacement with a sweeping input signal.

This difference means that the dynamic characteristic of the mold oscillator changes according to operating conditions; i.e., an unknown non-linear force term α must be introduced to enable Eq. (1) to follow the oscillating input signal (Eq. (2)):

$$m\ddot{y} + c\dot{y} + (k_{leaf} + k_{add})y - k_{leaf}\, y_{leaf} \neq F_{pressure} - mg \longrightarrow$$
$$m\ddot{y} + c\dot{y} + (k_{leaf} + k_{add})y - k_{leaf}\, y_{leaf} = F_{pressure} - mg + \alpha \tag{2}$$

A combination of factors, including variations in stiffness and damping ratio, friction between the piston and the cylinder, operating fluid leakage, and structural characteristics, causes the unknown force.

2.1.2. Dynamic analysis of experimental data about displacement and pressure

A sweeping input signal was applied, and the dynamics response was converted to the frequency domain. Peak pressure force and displacement frequencies were related to excitation frequencies 1~7 Hz (Table 2). However, unlike the step input signal, high peak frequencies of 43~49 Hz were found in the displacement's fast Fourier transform (FFT). Because ω_{exc} is an excitation oscillation and the harmonic terms are local vibrations, these terms correspond to friction, stiffness, and damping ratio variation proportional to the excitation oscillation. The harmonics terms can be simplified as when $f = 1$ Hz. The harmonics are all $1 + 2n$, $n = 1$; for $f > 1$ Hz, they are all nf, $n = 1$ in pressure.

Table 2. FFT of the pressure and displacement.

Excitation frequency [Hz]	Pressure	
	Excitation and harmonic terms [Hz]	High [Hz]
1	1/3/5/7/9/11···	·
2	2/4/6/8/10/12 ···	·
3	3/6/9/12/15/18 ···	·
4	4/8/12/16/20/24 ···	·
5	5/10/15/20/25/30 ···	·
6	6/12/18/24/30/36 ···	·
7	7/14/21/28/35/42 ···	·
Excitation frequency [Hz]	Displacement	
	Excitation and harmonic terms [Hz]	High
1	1/3/5/7/9/11···	49
2	2/4/6/8/10/12 ···	48
3	3/6/9/12/15/18 ···	47
4	4/8/12/16/20/24 ···	46
5	5/10/15/20/25/30 ···	45
6	6/12/18/24/30/36 ···	44
7	7/14/21/28/35/42 ···	43

Also, all High frequencies = 50 – f in displacement. However, additional peak frequencies 43~49 Hz are not proportional to ω_{exc}; all of these frequencies are $(50 - \omega_{exc})$ Hz. This relationship indicates that the structural characteristics of the support part or functional component are changed.

2.1.3. Definition of the non-linear force

The mold's displacement, velocity, and acceleration (Fig. 4) were derived by direct numerical integration using the Park stiffly stable method based on the experimental mold displacement. [23] Unlike the velocity and acceleration of a sine function, the velocity and acceleration of the mold include beat phenomena (Section 4).

By substituting this motion into Eq. (3), the unknown force α can be identified as a sine distribution (Fig. 5). To formulate a mathematical model, the equation of motion is modified with a function with the same distribution as α.

$$m\ddot{y} + c\dot{y} + (k_{leaf} + k_{add})y - k_{leaf}\,y_{leaf} = F_{pressure} - mg + \alpha$$
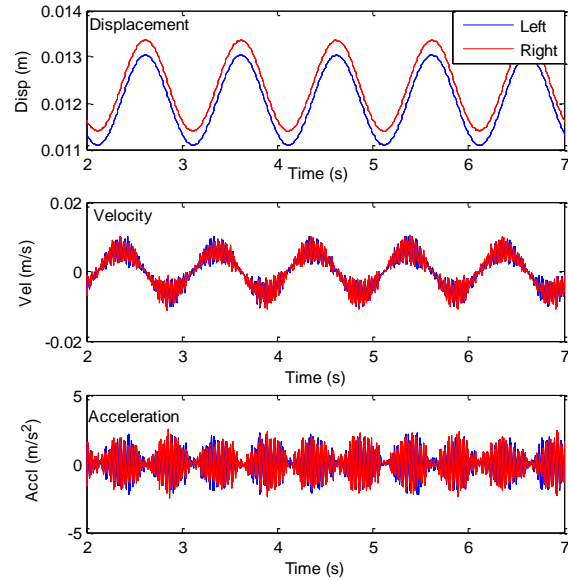(3)

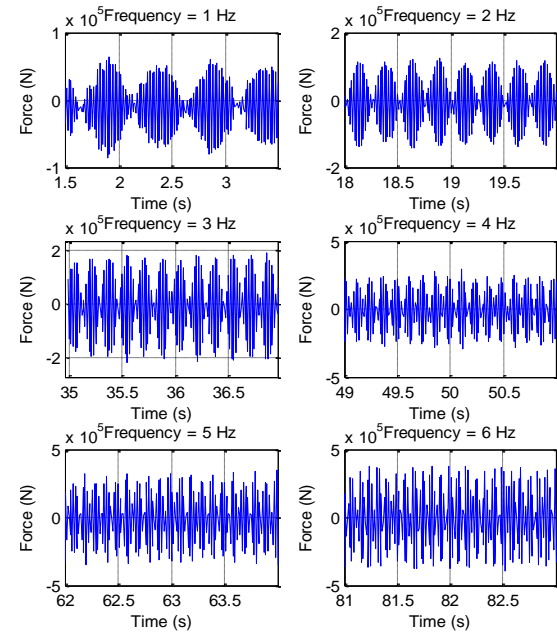**Fig. 4.** Dynamic behavior of the mold oscillator with 1 Hz excitation.

Fig. 5. Unknown force terms at different excitation frequencies.

2.1.4. The non-linear force distribution according excitation conditions

This section separates the unknown force into the excitation conditions and defining a summation of a Fourier series and a beat function to represent α (Fig. 6).
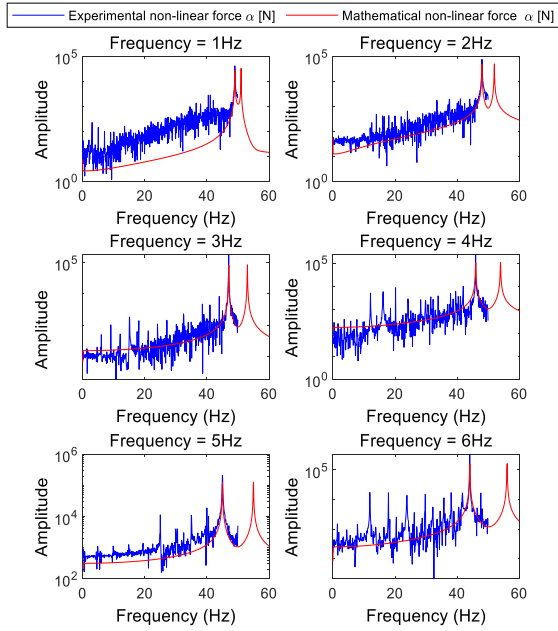
Fig. 6. FFT of the non-linear force α of the beat function and experimental data.

Due to the time step limitation in the experiment, 0.01 s, experimental α cannot be shown over 50 Hz. The Fourier series is used to represent the center line of α. The Fourier function has $1 \leq \omega_{exc} \leq 6$ Hz and harmonic terms (Table 3). The center value α_o is steady at all ω_{exc}. This value corresponds to 1.0355 tons. The stroke increased gradually over $1 \leq \omega_{exc} \leq 4$ Hz but increased and decreased dramatically at $\omega_{exc} = 5$ Hz and $\omega_{exc} = 6$ Hz. This distribution is correlated to the excitation conditions and the structural characteristic. In practice, the mold oscillator has a second torsional natural mode along its longitudinal axis, and this mode imparts an unbalanced force on left and right hydraulic cylinders at $\omega_{exc} \sim 5$ Hz.

Table 3. Fourier series for the unknown force with different excitation frequencies.

Frequency [Hz]	$f = a_o + a_1\cos(\omega t) + b_1\sin(\omega t)\cdots$ $+ a_2\cos(2\omega t) + b_2\sin(2\omega t)\cdots$ $+ a_n\cos(n\omega t) + b_n\sin(n\omega t)$		
	a_o [N]	max(f)-min(f)[N]	ω [Hz]
1	-10135.53	4191.30	1
2	-10199.31	7190.19	2
3	-10159.95	10345.57	3
4	-10198.77	11968.35	4
5	-10255.62	59333.70	5
6	-10252.26	5301.57	6

Except for the Fourier series force, the center line of α is 0. The beat function varied with ω_{exc} (Table 4); the amplitude of the beat function was proportional to the excitation frequency. The beat function showed two peak frequencies corresponding to $(50 \pm \omega_{exc})$ Hz. These results indicate that frequency analysis, including all design variables, should be considered. The following Section will analyze this phenomenon in detail. The mathematical expression and the experiment data about unknown force α were similar in frequency and amplitude but differed slightly in phase (Fig. 7); this difference can be corrected mathematically.

Table 4. Beat function for the unknown force with different excitation frequency.

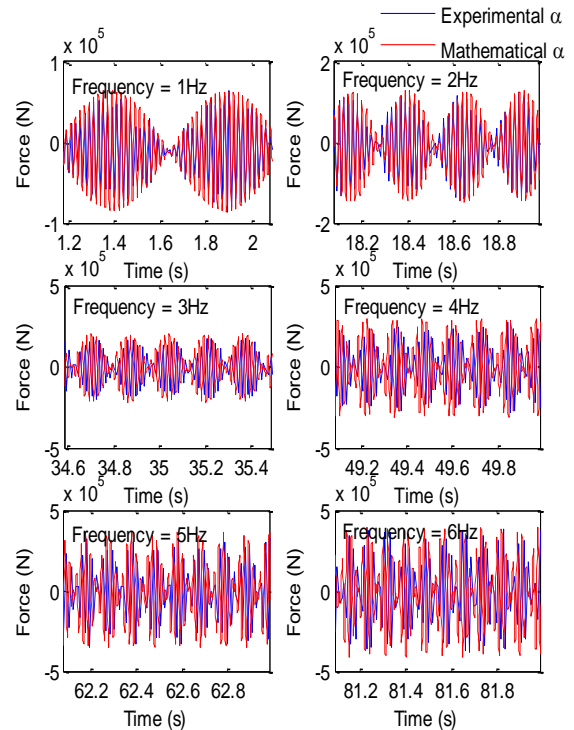| Frequency [Hz]	$f_{beat} = F_o \cos\left(\dfrac{\delta t}{2}\right)\cos\left(\dfrac{(\omega+\delta)}{2}t\right)$		
	F_o[N]	ω [Hz]	δ [Hz]
1	75236.49	97.94	2
2	138166.37	95.92	4
3	207682.21	94	6
4	302004.08	91.9	8
5	352677.60	89.9	10
6	400450.39	88.12	12

Fig. 7. Comparison between the experimental force α and the mathematical expression.

2.2. Analysis methodology with the modified mathematical model

2.2.1. The Natural characteristic of the mold oscillator

The mold oscillator includes four leaf springs at different locations (Fig. 8). In the 1-DOF equivalent model, all elastic components are regarded as one spring stiffness and are combined into one stiffness value. However, the system has different natural modes due to structural characteristics. A FE multi-body dynamics model is made to verify this fact, and the relationship between input and output experimental data is verified. The distribution of ω_{nat} produced by this model includes many ω_{nat} near 47 Hz (Fig. 9).

Generally, natural frequencies that are very close are generated by the same component, here probably the leaf spring. The leaf spring behaves as a beam and has several natural modes near 47 Hz in practice. The inertia of the moving weight and the mold influences this ω_{nat}.
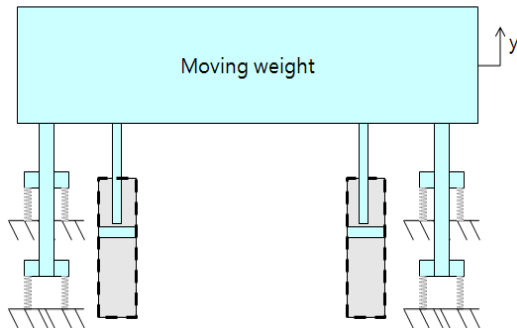

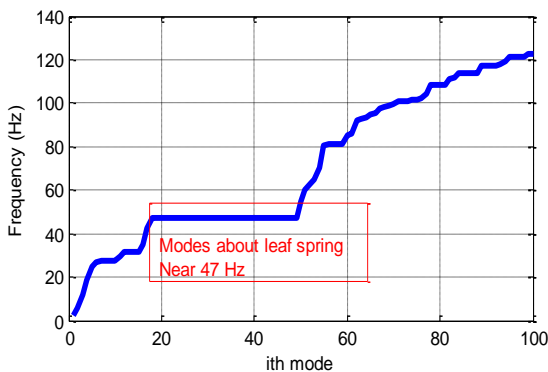**Fig. 8.** Design of the mold oscillator, including leaf springs.

Fig. 9. Natural frequency distribution of the mold oscillator.

The oscillating mechanism according to control processes should be considered. The pressure and displacement are input and output signals, respectively. The output signal includes information about the input, but the peak frequencies of the output at 49, 48, 47, 46, 45, 44, and 43 Hz are not dependent on the input; i.e., they must be caused by some other source. In the 1-DOF equivalent model, the additional peak frequencies 43~49 Hz, except for ω_{nat} and ω_{exc}, cannot be represented. Mechanical system modeling expands the model to a 2-DOF mass-damper-spring system that includes the structural characteristic.

2.2.2. 2-DOF mold oscillator model

The 2-DOF mass-damper-spring system for analysis of the beat phenomenon includes moving weight m_1 and the support m_2 of the moving weight, as shown in Fig. 10. The leaf spring is located between m_1 and m_2 and changes according to the excitation conditions. Without deflection of m_2, the additional peak frequencies at 49, 48, 47, 46, 45, 44, and 43 Hz cannot be acquired (Section 3.2). Eq. (4) is the equation of the 2-DOF model.

$$\begin{bmatrix} m_1 & 0 \\ 0 & m_2 \end{bmatrix}\begin{Bmatrix} \ddot{y}_1 \\ \ddot{y}_2 \end{Bmatrix} + \begin{bmatrix} c_1 + c_{leaf} & -c_{leaf} \\ -c_{leaf} & c_{leaf} + c_3 \end{bmatrix}\begin{Bmatrix} \dot{y}_1 \\ \dot{y}_2 \end{Bmatrix}$$
$$+ \begin{bmatrix} k_1 + k_{leaf} & -k_{leaf} \\ -k_{leaf} & k_{leaf} + k_3 \end{bmatrix}\begin{Bmatrix} y_1 \\ y_2 \end{Bmatrix} = \begin{Bmatrix} F \\ 0 \end{Bmatrix} \tag{4}$$
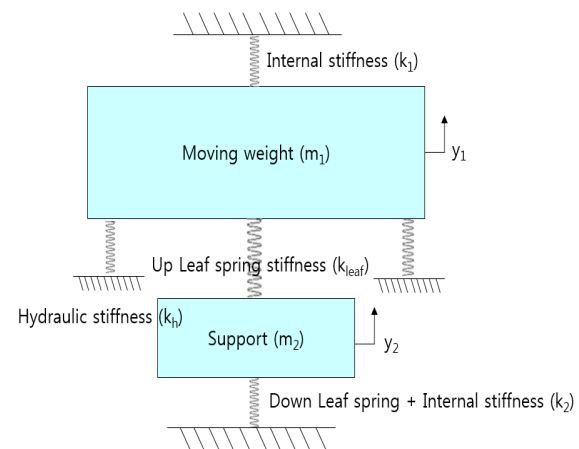

Fig. 10. Diagram of the modified mold oscillator model, including internal variable stiffness.

2.2.3. The leaf spring's stiffness variation according to excitation conditions

The additional peak frequency near 50 Hz changed according to excitation conditions in the experimental data. This phenomenon is that stiffness varies. Mechanical system modeling defines the mass m_1 and m_2 as 33 tons and 7 tons using the FE multi-body dynamics model. Even though peak frequencies exist during 1 Hz excitation locally, 1 Hz and 49 Hz frequencies are selected to check general dynamic behaviors. The beat period is 0.5 s (= 2 Hz), so the system must have 49-Hz and 51-Hz natural frequencies. To include 49-Hz vibration on m_1, m_1, and m_2 are given 51-Hz and 49-Hz ω_{nat}, respectively. In this problem, k_{leaf} and k_2 are design variables. The stiffness distribution varied with the excitation conditions (Table 5). As ω_{exc} increased, k_{leaf} increased, and k_2 decreased. This result is due to the leaf spring's natural mode and the adjoining stiffness, which consists of the damping ratio and the stiffness of the hydraulic cylinder.

3. Results and discussion

3.1. Dynamic analysis using the 1-DOF mold oscillator model considering the non-linear force

Numerical analysis simulated the 1-DOF model with external force, including α. Simulations considered a sine sweeping oscillation with $a = 2$ mm and $1 \leq \omega_{nat} \leq 7$ Hz. The numerical solution and the experimental data agreed well, except for a phase difference (Fig. 11), which is irrelevant in this analysis. The FFT (Fig. 12) of the displacement and pressure data reveal a 1st $\omega_{nat} = 2.499$ Hz in the pressure FFT. The natural frequency is the *y*-vertical translational mode.

Table 5. Leaf spring stiffness k_{leaf} and internal deformation stiffness k_2 according to excitation frequency.

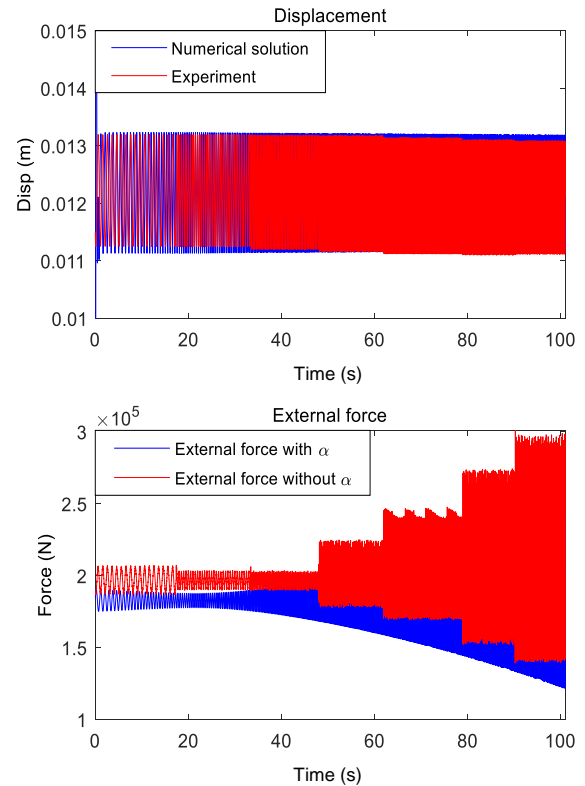| Frequency [Hz]	k_1 [N/m]	k_{leaf} [N/m]	k_2 [N/m]
1		70,815,413.66	680,000,000
2		120,815,413.7	600,000,000
3	3,300,000,000	175,815,413.7	540,000,000
4		230,815,413.7	470,000,000
5		290,815,413.7	410,000,000
6		350,815,413.7	340,000,000

Fig. 11. Comparison between the model and experiment about displacement and external force.
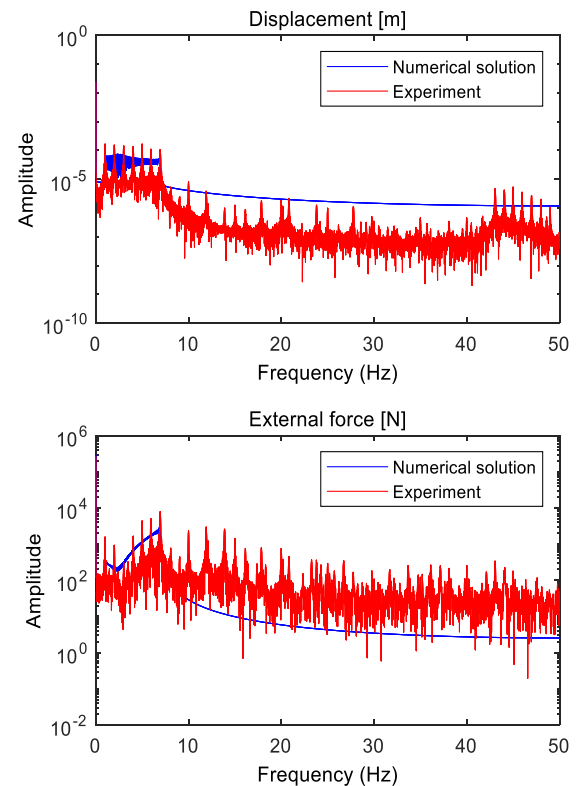

Fig. 12. FFT of the displacement and external force.

However, the 1-DOF model does not generate beats at 49, 48, 47, 46, 45, 44, and 43 Hz. According to this result, finding a suitable design using a detailed system, such as increases in the degree of freedom and mathematical expression for environmental conditions, is essential.

3.2. *Dynamic analysis using the 2-DOF mold oscillator model considering the leaf spring's stiffness variation*

Numerical analysis acquired the dynamic behavior of the time-frequency domain by using the 2-DOF model. Simulation conditions are the same as for the 1-DOF model. The numerical response and the experimental data are compared after the application of $\omega_{exc} = 1$ Hz (Fig. 13) and $\omega_{exc} = 6$ Hz (Fig. 14).
The simulated dynamic behavior of m_1 is similar to the experimental measurements. The phase difference between Moving weight and experiment data is input forcibly to show their similarity in detail. Additional peak frequency pairs are observed at 49 and 51 Hz, 48 and 52 Hz, 47 and 53 Hz, 46 and 54 Hz, 45 and 55 Hz, and 44 and 56 Hz (Fig. 15). However, the external force on the 2-DOF model is much higher than the experimental pressure force.
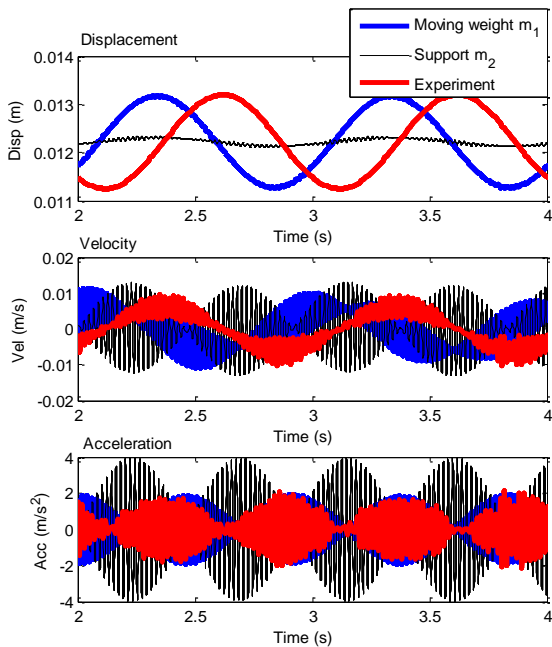

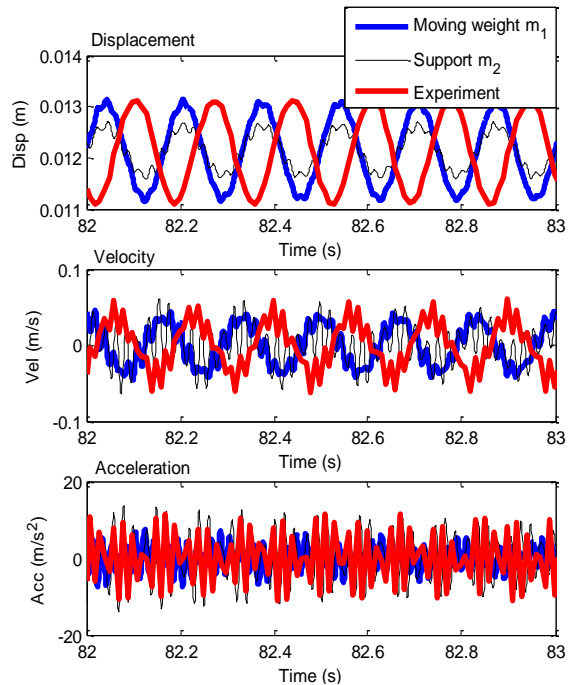**Fig. 14.** Dynamic behavior comparison between 2-DOF model and experiment with 2 Hz.

Fig. 13. Dynamic behavior comparison between 2-DOF model and experiment with 1 Hz.
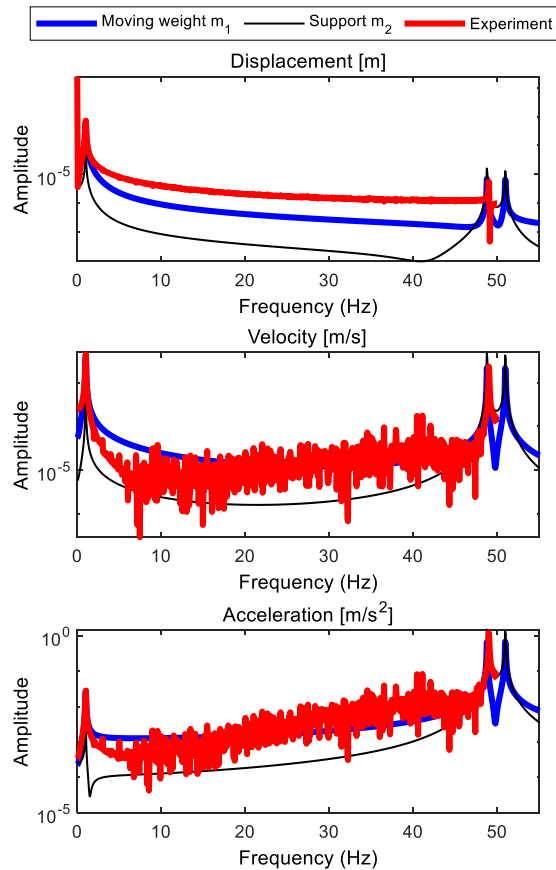

Fig. 15. FFT of dynamic behaviors with 1 Hz.

This difference occurred because m_1 and m_2 are chosen arbitrarily, so the stiffness is too high to fit target ω_{nat}; i.e., design variables should be adjusted to have same external force as the experimental force. Finally, This mathematical equation can conclude the mold oscillation as the summation of the (dominant) ω_{exc}; x_1 and local vibrations; x_2 (Fig. 16). The local vibrations, x_2, have weaker amplitudes than does dominant ω_{exc}; x_1. However, the local vibrations still happen in actual operation. When the local vibrations correspond to arbitrary natural modes of the mold oscillator, failure or quality defect, such as mold oscillation marks, can happen without warning; therefore, the system must be designed to minimize or change the local vibrations.

4. Conclusions

In this paper, the non-linear effect of the hydraulic cylinder on the mold oscillator is investigated numerically. The 1-DOF and 2-DOF mass-damper-spring models are simulated as with the experiment. To validate the model, the monitoring system measured the mold displacement and the hydraulic cylinder pressure with step and sine-sweeping excitation. The non-linear force is expressed as a summation of the Fourier series and the beat function using inverse dynamics to calculate velocity and acceleration from the displacement data. A comparison of the experiment and numerical solution and mathematical formulation of the non-linear effect indicates how to improve the accuracy control of the mold oscillator by using the present research. The study of the mold oscillator with different operating conditions indicates the following results:

(1) The unknown non-linear force α is a bulk variable that includes the effects of friction, stiffness variation, and various natural modes of the leaf spring effect that the FE multi-body dynamics model cannot demonstrate. Therefore, a mathematical model for control needs to apply α based on the operating condition to estimate the mold oscillator's status precisely.

(2) The beat period depends on the oscillating frequency and is presented as two peak frequencies around 50 Hz.
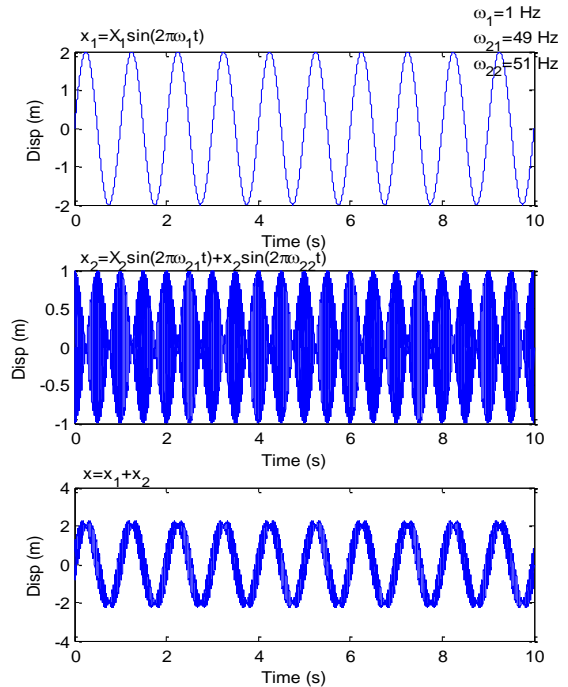

Fig. 16. Summation of global and local vibration.

(3) The modified mathematical model can give a basic guideline for the mold oscillator to estimate dynamic characteristics. However, the fact that the dynamic characteristic of the hydraulic servo system is sensitive to the oscillating condition means that our model should be used only in restricted conditions. In the future, Multi-Domain Modeling will combine our mechanical model with a linearized hydraulic servo system and analyze the sensitivity of the combination to design variable variation and design modification.

Acknowledgment

References

[1]   X. Z. Zhang, X. R. Zheng, Q. G. Liu, X. K. Li, and Y. M. Fang, "Investigation and application of non-sinusoidal oscillation technique of mold", *J. Iron. Steel Res. Int.*, Vol. 20, No. 12, pp.19-24, (2013).

[2]   L. Zhang, "Elastic vibration research of the non-sinusoidal oscillation system for the mold of continuous casting", *Proc. of 2011*

International Conference on Electronic & Mechanical Engineering and Information Technology, Vol. 6, Harbin, China, pp. 2920-2923, (2011).

[3]   Y. H. Park and H. Park, "Dynamic characteristic analysis of mold oscillator including improved gear mesh model and cam profile for eccentric shaft", *J. Mech. Sci. Technol.*, Vol. 28, No. 11, pp. 4465-4473, (2014).

[4]   W. Li, Y. Zhang, L. Yu, and J. Xiao, "Mold non-sinusoidal oscillating mode analyse and control of continuous casting machine", *Proc. of 2009 9th International Conference on Electronic Measurement & Instruments*, Beijing, China, pp. 567-570, (2009).

[5]   Y. H. Park and H. C. Park, "Dynamic characteristic analysis of hydraulic servo system in a mold oscillating mechanism", *Advanced Materials Research*, Vol. 1025-1026, pp. 183-191, (2014).

[6]   L. Smutný, R. Farana, A. Vítecek, and D. Kacmár, "Mould Level Control for the Continuous Steel Casting", *IFAC Proceedings Volumes*, Vol. 38, No. 1, pp. 163-168, (2005).

[7]   C. Liu and H. Jiang, "A seventh-order model for dynamic response of an electro-hydraulic servo valve", *Chin. J. Aeronaut.*, Vol. 27, No. 6, pp. 1605-1611, (2014).

[8]   B. G. Thomas, "On-line detection of quality problems in continuous casting of steel". *Proc. of Modeling, Control and Optimization in Ferrous and Nonferrous Industry, 2003 Materials Science and Technology Symposium*, Chicago, United States, pages 29-45, (2003).

[9]   J. Ni and L. Peng, "Nonlinear modeling and control for electro hydraulic servo system in pipe expanding process", *Proc. of the 48h IEEE Conference on Decision and Control (CDC) held jointly with 2009 28th Chinese Control Conference*, Shanghai, China, pp. 6034-6039, (2009).

[10]   X. D. Wang, M. Yao, L. Zhang, X. B. Zhang, and S. H. Chen, "Optimization of oscillation model for slab continuous casting mould based on mould friction measurements in plant trial", *J. Iron. Steel Res. Int.*, Vol. 20, No. 1, pp. 13-20, (2013).

[11]   H. J. Shin, G. G. Lee, S. M. Kang, S. H. Kim, W. Y. Choi, J. H. Park, and B. Thomas, "Effect of mold oscillation on powder consumption and hook formation in ultralow-carbon steel slabs", *Iron Steel Technol.*, Vol. 2, No. 9, pp. 56-69, (2005).

[12]   O. Angatkina, V. Natarajan, Z. Chen, M. Ding, and J. Bentsman, "Modeling and control of resonance effects in steel casting mold oscillators", *Acta Mechanica*, Vol. 230, pp. 2087-2104, (2019).

[13]   C. Zhou, X. Zhang, F. Wang, and Y. Fang, "Mold Oscillating System with Optimized Non-Sinusoidal Oscillation Profile", *Metallurgist*, Vol. 63, pp. 585-597, (2019).

[14]   M. Y. Coskun, and M. İtik, "Intelligent PID control of an industrial electro-hydraulic system", *ISA transactions*, (2023).

[15]   Z. Yan, "Characteristics of high energy-efficient Electro-hydraulic power source driven by servo motor and variable pump", *Proceedings of the Institution of Mechanical Engineers, Part C: Journal of Mechanical Engineering Science*, Vol. 237, No. 7, pp. 1525-1536, (2023).

[16]   X. J. Zhang, "Simulation and study on non-sinusoidal oscillation control system of continuous casting mold", *Proc. of Advanced Engineering Forum*, Shenyang, China, Vol. 2-3, pp. 53-56, (2011).

[17]   X. Yin and W. Chen, "Trends and development of steel demand in China: A bottom–up analysis", *Resour. Policy*, Vol. 38, No. 4, pp. 407-415, (2013).

[18]   A. Negahban and J. S. Smith, "Simulation for manufacturing system design and operation: Literature review and analysis", *J. Manuf. Syst.*, Vol. 33, No. 2, pp. 241-261, (2014).

[19]   M. Yellishetty, P. G. Ranjith, and A. Tharumarajah, "Iron ore and steel production trends and material flows in the world: Is this really sustainable?", *Resour. Conserv. Recycl.*, Vol. 54, No. 12, pp. 1084-1094, (2010).

[20]   B. Mochnacki and E. Majchrzak, "Sensitivity of conti-casting process with respect to cooling conditions", *J. Theor. Appl. Mech.*, Vol. 40, No. 1, pp. 129-147, (2002).

[21]   A. Y. Tsuprun, A. V. Fedosov, V. V. Kislitsa, and D. V. Pashchuk, "Study of the effect of the characteristics of harmonic mold-oscillation regimes on the surface quality of continuous-cast ingots", *Metallurgist*, Vol. 56, No. 7, pp. 498-503, (2012).

[22]   X. Yan, Y. Wang, Y. Luo, and Q. Wang, "Sensitivity analysis of torsional vibrations in mill drive train system", *Proc. of 2011 IEEE International Conference on Information and Automation*, Shenzhen, China, pp. 290-294, (2011).

[23]   K. C. Park, "An improved stiffly stable method for direct integration of nonlinear structural dynamic equations", *J. Appl. Mech.*, Vol. 42, No. 2, pp. 464-470, (1975).

How to cite this paper:

Y. H. Park, "Dynamic analysis of multi-body dynamics model of mold oscillator including self-excitation of supporting system,", *J. Comput. Appl. Res. Mech. Eng.,* Vol. 13, No. 2, pp. 229-239, (2024).

DOI: 10.22061/JCARME.2023.9238.2237

URL: https://jcarme.sru.ac.ir/?_action=showPDF&article=1996